2014 International Conference on Unmanned Aircraft Systems (ICUAS)
May 27-30, 2014. Orlando, FL, USA

Linear controllers implementation for a fixed-wing MAV

T. Espinoza[1], R. Parada[1], A. Dzul[1], and R. Lozano[2]

Abstract— **This paper deals with the experimental validation of linear controllers for a fixed-wing Miniature Air Vehicle (MAV). We are interested to realize a comparative analysis of two linear controllers, Proportional Integral Derivative (PID) and Proportional Derivative (PD), in order to know what controller has a better performance when they are used on an autonomous flight (altitude, yaw and roll). Experimental results are obtained in order to analyze the controllers and validate the performance of the fixed-wing MAV in presence of perturbations like wind gusts.**

Keywords: linear control, airplane model, embedded system, fixed-wing MAV.

I. INTRODUCTION

The term miniature air vehicle, which is commonly denoted by the acronym MAV, is used to refer the class of fixed-wing aircrafts with wingspans less than 5 feet. MAVs are typically battery powered, hand launched and belly landed, and therefore do not require a runway for take off or landing [1]. They are designed to operate from 20 minutes to several hours. Payloads range from ounces to several pounds. The small payload severely restricts the sensor suite that can be placed on MAVs, and also restricts the computer that can be put on board. These restrictions pose interesting challenges for designing autonomous modes of operation [1]. Thus, in the last years the study and analysis of nonlinear control theory, applied to Unmanned Aerial Vehicles UAV's, have increased in order to solve specific constraints (payload, operating time, etc.). These aerial systems have a large number of applications. Some examples of these applications are: monitoring disaster areas, localization of victims, infrastructure inspection for inaccessible locations, tasks of surveillance and photography. These important applications can be realized by using MAV formation, or MAV path following, or MAV trajectory tracking [1], [2]. All applications are obviously related with one of the MAV's characteristics: avoid risks to pilots and crew when flight conditions have low visibility or bad weather [3].

In this paper, we have implemented two linear controllers in a fixed-wing MAV in order to analyze the flight behaviour when is applied a PID control or a PD control. Given that it is a experimental validation, the presence of wind gusts has added a real constraint which is not present in simulations. In this sense, it is very important to know what type of control law is appropriate to be implemented in real weather conditions. On the other hand, It is well known that the obtention of the aerodynamic model represents a main part on the development of the system control law. Concerning aerial vehicles, a bad model obtention could lead to the MAV crash, even if the vehicle is placed a few meters of the ground [5], [6].

Then, the flying qualities of MAVs are just as important as they are for piloted aircraft, although envelope boundaries may not be quite the same, but they will be equally demanding. Thus, the theory, tools and techniques described in [5] or [6] can be applied to the analysis of the flight dynamics of fixed-wing MAVs [1]. If the task of a control system involves large range and/or high speed motions, nonlinear effects will be significant in the dynamics and a robust control may be necessary to achieve the desired performance [7], as in the case of the fixed-wing MAV control, where we could find a lack of information, a model inaccuracy and/or external disturbances [8]. In order to improve these disadvantages, a PID control law have been implemented to prove the robustness of this control law [4]. The linear controllers were

[1]Tadeo Espinoza, Ricardo Parada and Alejandro Dzul are with División de Estudios de Posgrado e Investigación, Instituto Tecnológico de la Laguna, 27000 Torreón, Coahuila, México dzul@faraday.itlalaguna.edu.mx

[2]Rogelio Lozano is with Heudiasyc Laboratory, Université de Technologiede Compiègne, Compiègne, UMR 7253, France rlozano@hds.utc.fr

applied to the decoupled dynamics of the airplane [6], [11], this is, each controller is applied in order to control the movements of altitude, yaw or roll. We developed an embedded system in order to compare and implemented these linear control techniques.

The paper organization is as follows: section II presents the mathematical model of the airplane; the section III deals with the control laws applied to the fixed-wing MAV; in section IV, we show the stability of the PD and PID controllers; in section V, we show the embedded system and the experimental results which have been obtained for the PID and PD controllers. Finally, section VI presents the conclusions and future work.

II. AIRPLANE MODEL

In order to obtain the model equations, by omitting any flexible structure of the MAV, the fixed-wing MAV is then considered as a rigid body. Also we do not consider the curvature of the earth, it is considered as a plane, because we assume that the fixed-wing MAV will only fly short distances. With the previous considerations, we obtain the model by applying the Newton's laws of motion.

A. Longitudinal dynamics

The parameters involved in the longitudinal dynamic model (1)-(5) are shown in Figure 1. These parameters allow to analyzing the movement toward the front of an airplane [5], particularly the altitude control.

$$\dot{V} = \frac{1}{m}(-D + T\cos\alpha - mg\sin\gamma) \quad (1)$$

$$\dot{\gamma} = \frac{1}{mV}(L + T\sin\alpha - mg)\sin\gamma) \quad (2)$$

$$\dot{\theta} = q \quad (3)$$

$$\dot{q} = \frac{M}{I_{yy}} \quad (4)$$

$$\dot{h} = V\sin(\theta) \quad (5)$$

where V is the magnitude of the airplane speed, α describes the angle of attack, γ represents the flight-path angle and θ denotes the pitch angle. In addition, q is the pitch angular rate (with respect to the y-axis of the aircraft body), T denotes the force of engine thrust, h is the airplane altitude [5] and δ_e represents the elevator deviation. The aerodynamic

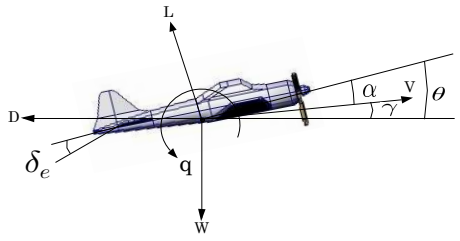

Fig. 1. Pure pitching motion

effects on the airplane are obtained by the lift force L and the drag force D. M is the pitching moment which acts on the airplane, m denotes the total mass of the airplane, g is the gravitational constant and I_{yy} describes the component y of the diagonal of the inertial matrix. The value of angle of attack is obtained by using the following relation $\alpha = \theta - \gamma$ [5]. The lift force L, the drag force D, and the pitching moment M are defined as [5]:

$$L = \bar{q}SC_L \quad (6)$$

$$D = \bar{q}SC_D \quad (7)$$

$$M = \bar{q}S\bar{c}C_M \quad (8)$$

where $\bar{q}$ denotes the aerodynamic pressure. S represents the wing platform area and $\bar{c}$ is the mean aerodynamic chord. C_D, C_L and C_M are the aerodynamic coefficients for drag force, lift force and pitch moment respectively

B. Lateral dynamic

The lateral dynamic generates the roll motion and, at the same time, induces a yaw motion (and vice versa), then a natural coupling exists between the rotations about the axes of roll and yaw [11]. In our case, to solve it, we have considered that there is a decoupling of yaw and roll movements [6]. Thus, each movement can be controlled independently. Generally, the effects of the engine thrust are also ignored [11]. In the Figure 2, the yaw motion is represented, which can be described with the following equations:

$$\dot{\psi} = r \quad (9)$$

$$\dot{r} = \frac{N}{I_{zz}} \quad (10)$$

$$\dot{V}_y = \frac{F_y}{m} - rV_x \quad (11)$$

$$\dot{V}_x = \frac{F_x}{m} + rV_y \quad (12)$$

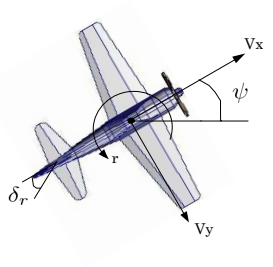

Fig. 2. Pure yawing motion

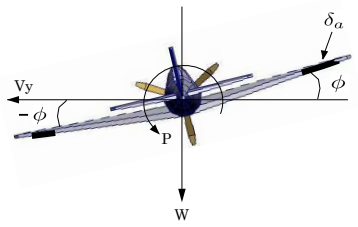

Fig. 3. Pure rolling motion

where ψ represents the angle of yaw and r denotes the yaw rate, with respect to the centre of gravity of the airplane, N is the yawing moment and I_{zz} represents the inertia in the z-axis. δ_r is the rudder deflection. V_x corresponds to the speed of the airplane in the longitudinal x-axis, V_y is the speed in the lateral y-axis, F_x describes the thrust force in the longitudinal x-axis and F_y denotes the component of the resultant lateral force on the y-axis. The equations related to the above forces and the yaw moment are [5].

$$F_x = \bar{q}SC_{x0} \quad (13)$$
$$F_y = \bar{q}SC_y \quad (14)$$
$$N = \bar{q}SC_n \quad (15)$$

where C_{x0}, C_y y C_n are the aerodynamic coefficients involved for the lateral dynamics. These coefficients are obtained by considering small angles and with low airplane speed. The following equations describe the dynamics for the roll motion:

$$\dot{\phi} = p \quad (16)$$
$$\dot{p} = \frac{\bar{L}}{I_{xx}} \quad (17)$$
$$\dot{V}_y = \frac{F_y}{m} + pV_x \quad (18)$$
$$\dot{V}_x = \frac{F_x}{m} - pV_y \quad (19)$$

where p denotes the roll rate, $\bar{L}$ is the rolling moment, I_{xx} represents the inertia for the x-axis and ϕ describes the roll angle. The aerodynamic effects on the airplane are obtained as they have been obtained in the yaw motion. In the Figure 3, it is observed that δ_a represents the deviation of the ailerons. In the case of the roll moment, this corresponds the expression $\bar{L} = \bar{q}SbC_L$, where b is the wing span of the airplane and C_L represents the aerodynamic coefficient of the roll moment [5].

III. LINEAR CONTROLLERS DESIGN

In this section, we describe the linear controllers that have been designed in order to control the fixed-wing MAV.

A. Altitude control

In order to design the altitude control law, we consider the equations defining the longitudinal dynamics, except the equation (1) which defines the linear longitudinal velocity, because it is considered to be constant; the equation (2) is not used, because it represents the flight-path angular rate. Then the aerodynamic model is defined as $\dot{\theta} = q$, $\dot{q} = C_{m_q}q + C_{m\delta_e}\delta_e$, where δ_e is the input control, and C_{m_q}, $C_{m\delta_e}$ are the aerodynamic coefficients. The altitude error has been defined as $\tilde{e}_h = h_d - h$, and it denotes the difference between the desired altitude h_d with respect to the current altitude h, where h is obtained by integrating (5). We have designed PD and PID controllers [9], [10]. The PD control is an immediate extension of the Proportional velocity feedback control, as its name suggests, the control law is not only composed of a proportional term of the position error as in the case of proportional control, but also of another term which is proportional to the derivative of the position, i.e. to its velocity error, $\dot{\tilde{e}}_h$. The PD control law for altitude motion is given by:

$$u = k_{pl}\tilde{e}_h + k_{vl}\dot{\tilde{e}}_h \quad (20)$$

where k_{pl} and k_{vl} are the positive constant gains of the PD controller. The fixed-wing MAV is affected for the gravity force, and in order to compensate

this, we apply a Proportional Integral Derivative control in order to drive the position error to zero [10]. This reasoning justifies the application of Proportional Integral Derivative (PID) control. The PID altitude control law is given by:

$$u = k_{pl}\tilde{e}_h + k_{il}\int_0^t \tilde{e}_h(\sigma)d\sigma + k_{vl}\dot{\tilde{e}}_h \qquad (21)$$

where k_{pl}, k_{il} and k_{vl} are respectively called as the position, integral and velocity gains of the PID controller. These gains are positive constants, where $l = h, \psi, \phi$ (we will use ψ and ϕ in the next linear controllers). We have realized several simulations in order to calculated the gain values by the second method of Ziegler-Nichols, with the aim of maintain the control law within of the allowed torque by the servomotors of the MAV fixed-wing, and then we did a series of fine tunings in the experimental test in order to get the desired response [9].

B. Yaw control

In order to design the control laws for the pure yawing motion, we only consider the aerodynamic model for yaw movement. Then, we exclude (11) and (12) because they link the lateral and longitudinal linear velocities generated by the yaw angle. The model has been then defined as $\dot{\psi} = r$, $\dot{r} = C_{n_r}r + C_{n\delta_r}\delta_r$, where δ_r is the input control, C_{nr} and $C_{n\delta_r}$ are the aerodynamic coefficients for the yaw movement.

For PD and PID controllers, we have used the general structures shown in (24) and (25), but now, obviously we define the yaw error as $\tilde{e}_\psi = \psi - \psi_d$, where ψ is obtained by integrating (9), and ψ_d denotes the desired yaw angle.

C. Roll control

In order to design the attitude linear control laws for the roll movement, we consider the equations that only define the roll motion, then we exclude (18) and (19), because they link the lateral and longitudinal linear velocities generated by roll angle. We can then write $\dot{\phi} = p$, $\dot{p} = C_{L_p}p + C_{L\delta_a}\delta_a$, where δ_a is defined as the control input and C_{L_p}, $C_{L\delta_a}$ are the aerodynamic coefficients for the roll movement.

For development of the roll control strategy, we apply the same structures as those used for the PD and PID controllers presented previously in (24) and (25). Let us define the roll angle error as $\tilde{e}_\phi = \phi - \phi_d$, where ϕ_d is the desired roll angle and ϕ is the current roll angle that is obtained by integrating the roll rate in equation (16).

IV. Stability of the classical PD and PID controller

This section presents the stability analysis of the classical PD and PID controllers when they are applied to the MAV.

A. Stability of the classical PD controller

Consider the next generalized dynamic equations:

$$\dot{x}_{1a} = x_{2b} \qquad (22)$$
$$\dot{x}_{2b} = c_1 x_{2b} + c_2 u \qquad (23)$$

where x_{1a} is the Euler angle defined in the airplane fixed frame, $a = \theta, \psi, \phi$ represents the pitch, yaw or roll angles respectively. x_{2b} is the angular rate, with $b = q, r, p$ as the angular rate of pitch, yaw or roll. Finally c_1 and c_2 are the aerodynamic coefficients. Defining the error as $\tilde{x}_{1a} = x_{1a} - x_{d_a}$, we assume that the desired position x_{d_a} is constant. Under this condition, the closed-loop equation may be rewritten in terms of the new state vector

$$\begin{bmatrix} \dot{\tilde{x}}_{1a} \\ \dot{x}_{2b} \end{bmatrix} = \begin{bmatrix} x_{2b} - \dot{x}_{d_a} \\ c_1 x_{2b} + c_2(k_{pa}\tilde{x}_{1a} + k_{va}\dot{\tilde{x}}_{1a}) \end{bmatrix}$$

The equilibrium point that will be studied is the origin of the state space, *i.e.* $[\dot{\tilde{x}}_{1a}, \dot{x}_{2b}]^T = 0$. Now, we use the Lyapunov direct method [10]. Consider the following Lyapunov function candidate

$$V(\tilde{x}_{1a}, \dot{x}_{2b}) = \frac{c_2}{2}k_{pa}\dot{\tilde{x}}_{1a}^2 + \frac{1}{2}x_{2b}^2$$

The total derivative of $V(\tilde{x}_{1a}, \dot{x}_{2b})$ yields

$$\dot{V}(\tilde{x}_{1a}, \dot{x}_{2b}) = c_2 k_{pa}\tilde{x}_{1a}\dot{\tilde{x}}_{1a} + x_{2b}\dot{x}_{2b}$$

Substituting the corresponding variables in $\dot{V}(\tilde{x}_{1a}, \dot{x}_{2b})$, and using the fact that c_1 and c_2 are negative constant values, we obtain

$$\dot{V}(\tilde{x}_{1a}, \dot{x}_{2b}) = -x_{2b}^2(c_1 + c_2 k_{va}) \qquad (24)$$

By the fact that $\dot{V}(\tilde{x}_{1a}, \dot{x}_{2b}) \leq 0$, from Theorem 2.3 of [10], we can conclude that the origin is

stable. We may try to apply La Salle's theorem (Theorem 2.7 of [10]) to analyze the asymptotic stability of the origin. To that end, notice that the set Ω is given by

$$\begin{aligned}\Omega &= \{x \in \mathbb{R} : \dot{V}(x) = 0\} \\ \Omega &= \{\tilde{x}_{1a}, \dot{x}_{2b} \in \mathbb{R} : \dot{V}(\tilde{x}_{1a}, \dot{x}_{2b}) = 0\}\end{aligned}$$

Observe also that $\dot{V}(\tilde{x}_{1a}, \dot{x}_{2b}) = 0$ if and only if $x_{2b} = 0$. We can see that the solution $x(t)$ belongs to Ω, for all $t \geq 0$, if $x_{2b}(t) = 0$ for all $t \geq 0$ (necessary and sufficient condition), and therefore $[\tilde{x}_{1a}(0), \dot{x}_{2b}(0)]^T = 0 \in \mathbb{R}$ is the only point of Ω. Thus, from La Salle's theorem, this is enough to establish global asymptotic stability of the origin.

B. Stability of the classical PID controller

We have used the Routh's stability criterion due to the complexities involved to demonstrate the stability of the PID controller by means of the Lyapunov direct method [10]. To apply this theory, we need to convert the system (22)-(23) in a transfer function, then the closed-loop of the system is given by

$$\frac{C(s)}{R(s)} = \frac{-c_2(-k_{pa}s^2 - k_{va}s - k_{ia})}{s^3 + (c_1 + c_2k_{va})s^2 + c_2k_{pa}s + c_2k_{ia}} \tag{25}$$

where k_{pa}, k_{va} and k_{ia} are the positive constant gains, then applying the Routh's stability criterion to the polynomial

$$s^3 + (c_1 + c_2k_{va})s^2 + c_2k_{pa}s + c_2k_{ia} = 0$$

the array of coefficients becomes

$$\begin{array}{ccc} s^3 & 1 & c_2k_{pa} \\ s^2 & c_1 + c_2k_{va} & c_2k_{ia} \\ s^1 & c_2k_{pa} - \frac{c_2k_{ia}}{c_1+c_2k_{va}} & \\ s^0 & c_2k_{ia} & \end{array}$$

The system will be stable, with the PID controller, if the next condition is satisfied:

$$c_2k_{pa} > \frac{c_2k_{ia}}{c_1 + c_2k_{va}} \tag{26}$$

that is, all roots have negative real parts.

V. Experimental results

In this section, we present the developed embedded system where the linear controllers will be tested, and the experimental results that we have obtained for each one of the cases under analysis.

A. Experimental fixed-wing MAV

The embedded system consists of a microprocessor rabbit RCM6000 which read the data from the Inertial Measurement Unit (IMU) and the radio signals. The used IMU corresponds with the MicroStrain 3DM-GX1, which give us the Euler angles and the angular rates that we need in the linear controllers design before. The radio control that is used to pilot and give the order of autopilot is the Futaba T7C (transmitter and receptor). We have used a wireless module in order to obtain all necessary data to compute and to graph the control law signals, this module is a XBee-PRO 802.15.4.

On order to get the altitude, we implemented the altimeter and the microcontroller Parallax, these systems are connected to rabbit RCM6000, see Figure 4. The airplane used is the T-28 Trojan whose technical characteristics are given in Table I.

Fig. 4. Embedded system on the experimental platform

Parameter	Value
Wingspan	1118 mm
Fuselage length	914 mm
Wing area	0.09 m^2
Weight approx	1500 g
RC functions	Aileron, elevator, rudder, throttle

TABLE I
PARAMETERS OF THE MAV

B. Altitude movement

Figure 5 shows the altitude behavior for different desired altitudes when the PD control law is applied. In the following figures, we use the

acronym AC in order to show when the Automatic Control is running, and the acronym MC means that the MAV is flying in Manual Control. We can observe that PD controller achieves its objective (solid line). The dashed line represents the desired altitude. In Figure 5, it is shown in solid line, the torque that has been used to reach the desired altitude signals. The torque has a zero value when the system is in open loop, this is, in manual control (MC). The same torque value will be also presented for the roll and yaw motions. The used gain values for the linear controllers are shown in Table I. The Figure 6 shows the PID control response to altitude movement, we can see some oscillations in its performance, this could be due to the integral action that is not required for this movement (when it is used the same values of the proportional and derivative gains), or we need to retune the PID control gains [9]. In order to obtain some comparisons, we have decided to keep the same values of the proportional and derivative gains of the PD control on the PID control law. (this criterion has been applied for the roll and yaw motions). The Figure 6 shows the applied torque for the PID control in altitude, we can see than it has almost the same magnitude with respect to the applied torque for the PD altitude control, except after second 80, where the PD control has an overshot (perhaps due to the wind gusts). By substituting the gains of the PID altitude control, shown in Table II, inside (26), it results that $10.81 > 0.0480$. This means that the system is stable. In (24), we have demonstrated that the origin is stable and by applying La Salle's theorem, we conclude the global asymptotic stability of the origin for the PD controller in altitude, yaw and roll movements.

C. Yaw movement

The Figure 7 shows the yaw signal behavior when the PD controller is applied (AC). The reference is shown in dashed line, and the yaw angle is shown in solid line. We can see, at the second and last time when the control law is applied, that the signal has been affected by the presence of wind gusts (denoted by WG), Figure 7, however the PD control keeps the desired reference value with a little steady state error. The Figure 7 shows, in solid line, the applied moments which are required to obtain the desired yaw angle (AC). We can observe some changes of sign in yaw angle (denoted by CS), Figure 7. This is due to the program algorithm that has been used in the embedded system, because it takes the IMU measurements on the range of $\pm 180^{\circ}$ in order to limit the yaw, roll and pitch motions.

$Altitude$	k_{ph}	k_{ih}	k_{vh}
PD	10	-	0.1
PID	10	0.005	0.1
Yaw	$k_{p\psi}$	$k_{i\psi}$	$k_{v\psi}$
PD	5	-	1
PID	5	0.01	1
$Roll$	$k_{p\phi}$	$k_{i\phi}$	$k_{v\phi}$
PD	5	-	1
PID	5	0.1	1

TABLE II
GAINS OF THE CONTROLLERS

In Figure 8, it is shown the PID control action for the yaw motion (AC). We can see that this fly test has been also perturbed by wind gusts (WG). However the PID controller try to keep the yaw angle nearer to desired reference, compared with respect to the PD control. The Figure 8 presents more changes of sign in yaw angle, should be mentioned that the yaw controllers are not affected for the change of sign (CS), long as the control law not be applied in that change of sign, this means, that we can activate the yaw controllers inside of $\pm 180^{\circ}$. We can observe that the PID control applies a lower torque, in order to keep the desired angle in presence of wind gusts (WG), than the PD control, Figure 8. The used gains values for yaw motion are presented in Table I. In order to demonstrate the stability of the PID controller which is applied to yaw movement, we substituting, in (26), the gains of the PID controller that are shown in Table II. The result is $299 > 0.0097$, and this means that the system is stable.

D. Roll movement

The Figure 9 shows the desired reference signal, in dashed line, and the roll angle, in solid line. For this case, the selected reference is zero, that is, because we want that the fixed-wing MAV does

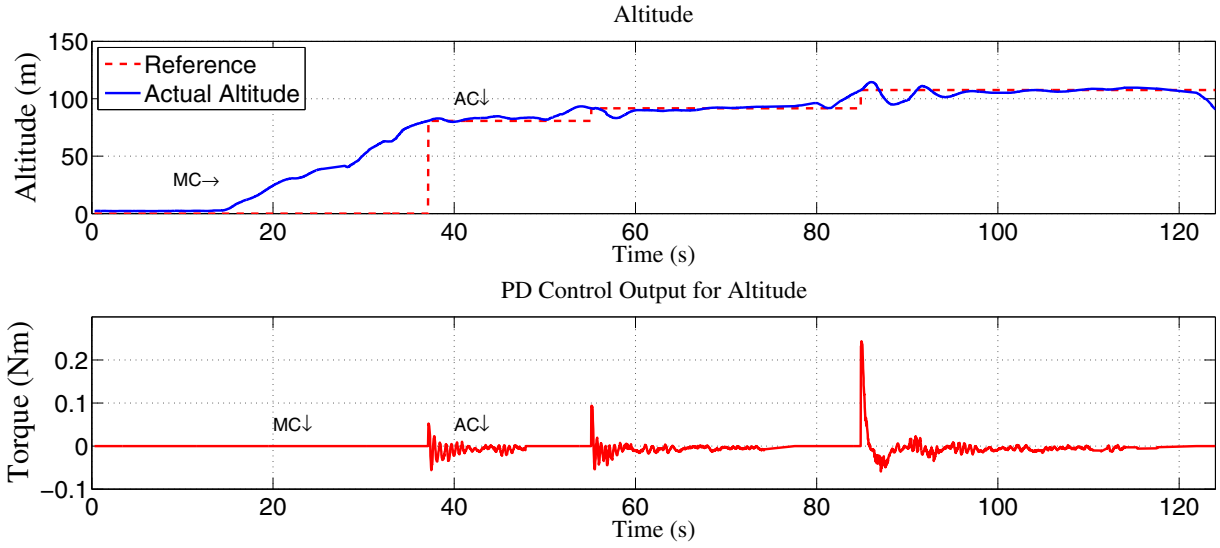

Fig. 5. PD control response for altitude

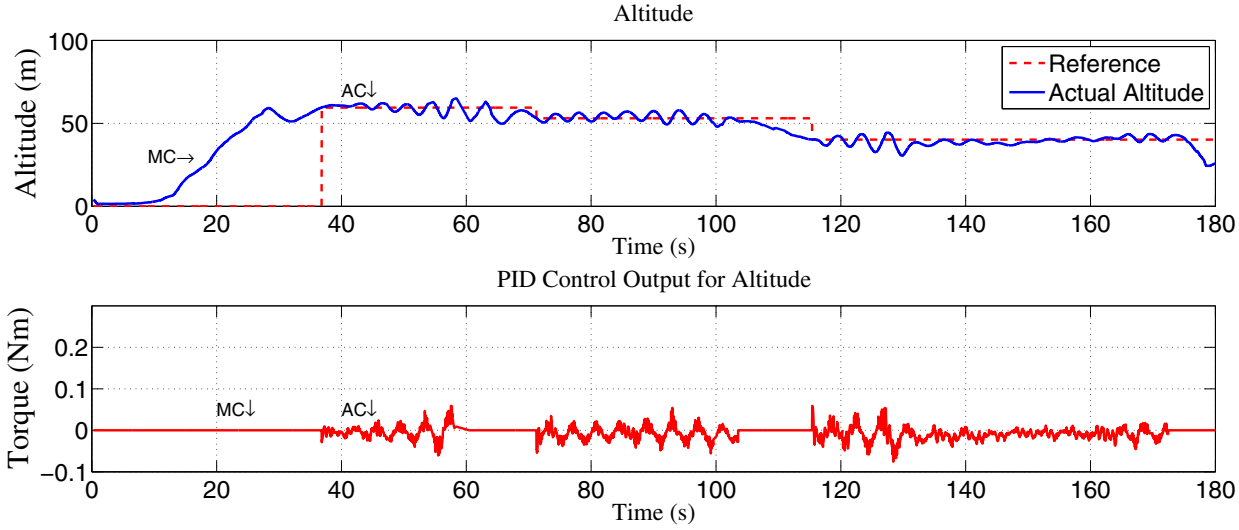

Fig. 6. PID control response for altitude

not carry out a turn. The PD control in roll motion presents a steady state error (AC), and we can see that, in presence of wind gusts (WG), the steady state error increases its magnitude, Figure 9. The used gains values, for the roll controllers, are presented in Table I. The Figure 9 also shows the applied torque for PD control in order to achieve the desired roll angle.

The Figure 10 shows the response of PID control, we can see that the steady state error is lower, compared with respect to the PD control, or almost zero. In presence of wind gusts (WG), the PID controller is trying to bring the roll angle to the desired reference. In the Figure 10, we can observe the applied torque of the PID control law in order to achieve the desired roll motion.

In order to demonstrate the stability of the PID controller which is applied to roll movement, we substituting, in (26), the gains of the PID controller for the roll movement that are shown in Table II. The result is $74.98 > 0.0392$, and then it means that the system is stable.

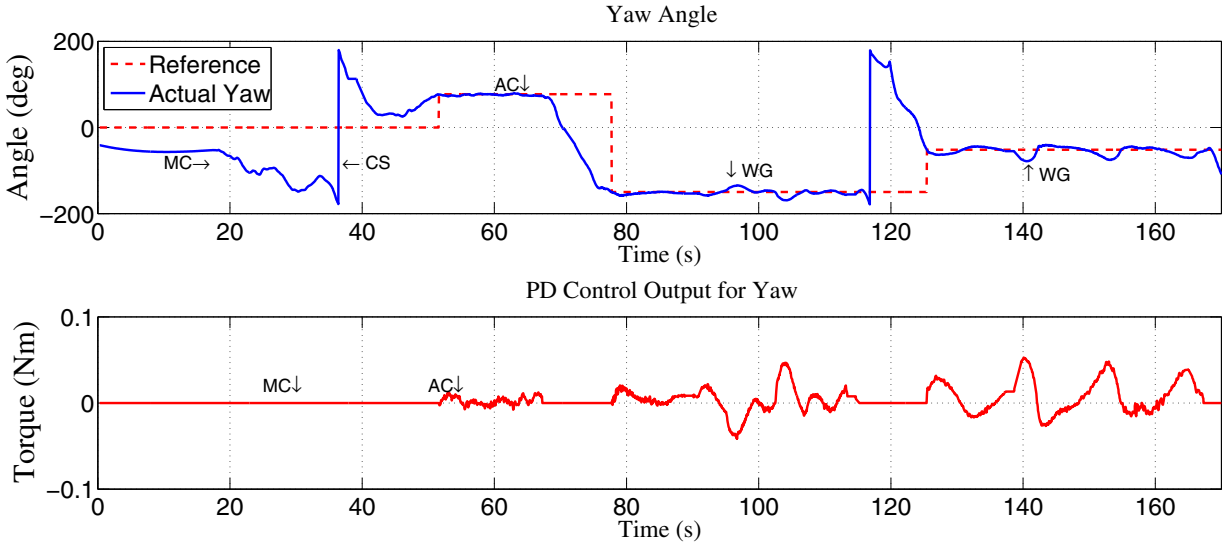

Fig. 7. PD control response for yaw motion

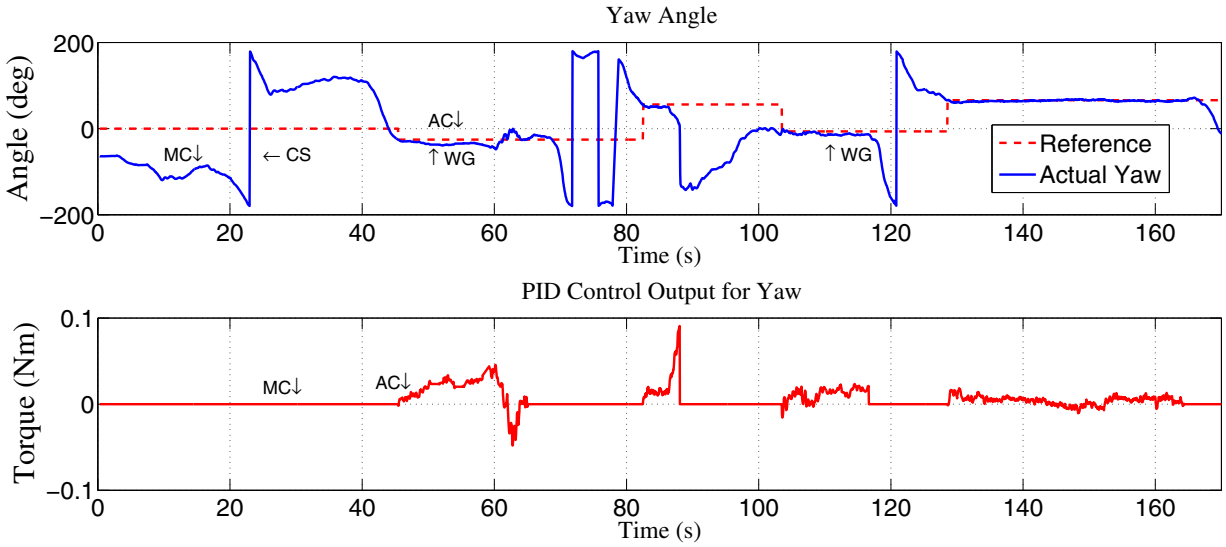

Fig. 8. PID control response for yaw motion

VI. Conclusions and Future Work

We present experimental results of the linear controllers implementation for a radio-controlled airplane (MAV platform). We have designed two linear controllers based on the PD and PID techniques, with the purpose of regulate the flight of a fixed-wing MAV. We have realized an analysis of such controllers in order to know which control law has a better performance. In the experimental results, we can observe that the PD and PID controllers have a good performance for each one of the three analyzed dynamics. The PD control has presented a steady state error in yaw and roll motion, and in presence of wind gusts, this error is bigger and applies more torque in order to regulate these perturbations, compared with respect to the PID controller. The PID control law, for yaw motion, shows a good response in presence of the wind gusts and it applies a lower torque than the PD control, in order to compensate these

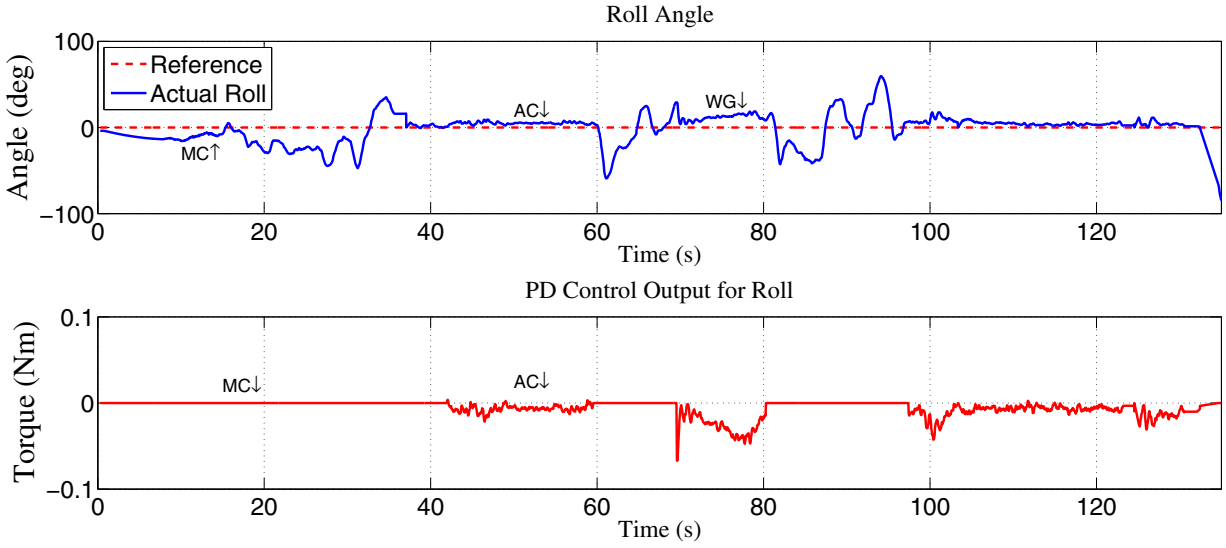

Fig. 9. PD control response for roll motion

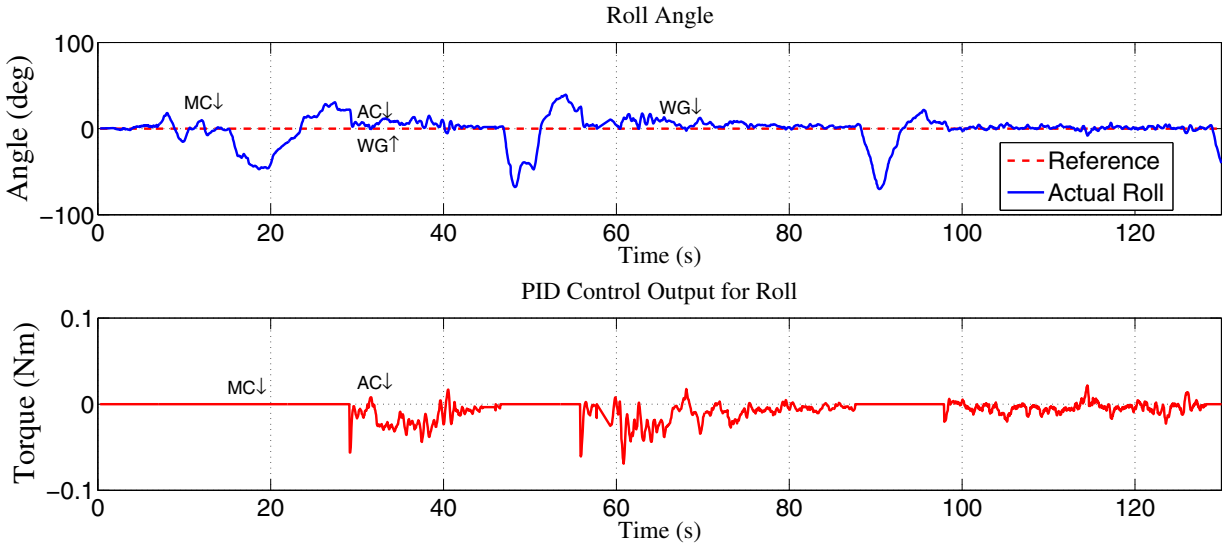

Fig. 10. PID control response for roll motion

perturbations.

The PD control, in roll motion, has the same state steady error like it is showed in yaw, but it also has a good performance in roll motion. The PID control has a very good performance in order to compensate the perturbations of the wing gusts and it eliminates the steady state error in roll motion.

In the case of the altitude control, we can observe that the PD control presents a very good performance in order to keep the desired altitude. The PID control, in altitude, presents some oscillations, this is due to the integral action that is not required for this movement (by maintaining the same values for the proportional and derivative gains). Before reaching this conclusion, we conducted several tests with different values of the integral gain, and we have finished by retuning the proportional and derivative gains if we search a better performance.

Our future work will consist in the implemen-

tation of linear robust controllers and nonlinear controllers in the MAV platform in order to get a better performance in presence of perturbations, like wind gusts.

REFERENCES

[1] R. W. Beard and T. W. Mclain, "Small Unmanned Aircraft", Ed. Princeton University Press, ISBN: 978-0-691-14921-9, 2010

[2] J. Guerrero and R. Lozano, "Flight Formation Control", Ed. Wiley, ISBN: 184-82-1323-9, 2012

[3] Kimon P. Valvanis, "Advances in Unmanned Aerial Vehicles", Ed. Springer, ISBN: 1-4020-6113-4, 2007

[4] M. Vagia, "PID Controller Design Approaches - Theory, Tuning and Application to Frontier Areas", Ed. InTech, ISBN 978-953-51-0405-6, 2012

[5] Brian L. Stevens and Frank L. Lewis, "Advances in Unmanned Aerial Vehicles", Ed. Jhon Wiley and Sons, ISBN: 0-471-61397-5, 1992

[6] M. V. Cook, "Flight Dynamics Principles", Second edition, Ed. Elsevier, ISBN: 978-0-7506-6927-6, 2007

[7] J.J. Slotine and W. Li, "Applied Nonlinear Control ", Ed. Prentice Hall, ISBN: 0-130-40890-5, 1991

[8] A. Levant, et al, "Aircraft Pitch Control Via Second Order Sliding Technique", AIAA Journal of Guidance, Control and Dynamics, 23(4), 586-594, 2000

[9] K. Ogata, "Modern Control Engineering", Ed. Prentice Hall, Fifth edition, New Jersey, ISBN: 0136156738, 2009

[10] R. Kelly and V. Santibáñez and A. Loría, "Control of Robot Manipulators in Joint Space", Springer, ISBN-10: 1852339942, 2005

[11] D. Mclean, "Automatic Flight Control Systems", Ed. Prentice hall International, ISBN: 0-13-054008-0, 1990

[12] O. Harkegard and S. T. Glad, "A Backstepping design for Flight Path Angle Control", In proceedings of the 39th Conference on Decision and Control, Sydney, Australia, 12-15 Dic, Page(s):3570 - 3575 vol.4, 2000